CST0018

Prediction and validation of underwater shock wave pressure generated by explosion and electrical discharge method

Paramet Suttiprapa, Wirapan Seehanam, and Kulachate Pianthong*

Department of Mechanical Engineering, Faculty of Engineering, Ubon Ratchathani University (UBU), 85 Sathonlamark Road, Warin Chamrap, Ubon Ratchathani 34190, Thailand

* Corresponding Author: k.pianthong@gmail.com

Abstract. Recently, the underwater shock wave (USW) is widely applied in many fields such as medical, biological, food, and industrial applications. The USW can be generated either by an underwater explosion or by the high voltage electrical discharge (HVED). However, in practices, the HVED is more practical and appropriate to apply in such fields, because it is repeatable and easier to control. This study aims to investigate characteristics and peak pressure of the USW generated by both methods by CFD simulations. Peak pressures generated by both methods are predicted and validated through explosive theory, experimental and CFD results. Due to the discharge phenomena is very difficult to simulate and its electro-hydraulic behavior is like the underwater explosion, therefore researchers like to study the USW by simulating the underwater explosion rather than underwater HVED. Therefore, the equivalent mass of TNT (W_t) obtained from the same peak pressure of electrical breakdown and explosive detonation is estimated and then becomes the input parameters for the CFD study. The HVED is generated by electrical discharge through electrodes gap being anode into cathode. Conditions of investigation in the CFD simulation are the electrical breakdown energy (E_b) ranged of 2.5-30kJ. The peak pressure at various distances from center of explosion point which are 345, 445, and 555 mm, respectively are predicted. It is found that peak pressure predicted by the CFD are in the range of 32-81 bar, 25-62.5 bar, and 20-49.9 bar, respectively. The error of peak pressure predicted by the CFD simulation compared to that from the theory of explosive detonation range is about 5-11%. Moreover, the results from the CFD simulation is also close to experimental result. Therefore, it is confirmed that the proposed method is reliable and effective to use to study of the USW. This method will be useful for further investigation or facility design.

1. Introduction

Nowadays, the underwater shock wave (USW) is widely used in many fields such as medical, biological, food, and industrial applications. Hosseini et al. (2011) studied the micro USW for medical application which generated by the shock wave generator. The peak pressure measured by the PVDF needle hydrophone and phenomena of USW was visualized by the time resolved high-speed shadowgraph visualization. In this study, it was concluded that the USW is suitable for precise medical procedures [1]. Alvarez et al. (2004) investigated the effect of the USW on inactivation of Escherichia coli O157:H7, Salmonella Typhimurium, and Listeria monocytogenes. It was found that an influence of the USW effected on E. coli O157:H7, S. Typhimurium, and L. monocytogenes [2]. Boussetta et al. (2009) researched the improvement of polyphenols extraction grape pomace using USW. The result found that the total polyphenols treated by the USW increase compared to the control experiment [3]. Maroušek (2014) proposed the novel technique to enhance the disintegration effect of the USW on oilseed. It was found that this technique may be increased the oil yield of extraction because the cell wall was broken by the USW [4]. Boussetta et al. (2012) investigated the USW assisted the polyphenols extraction from grape pomace. It found that the USW are effectives for the polyphenols extraction from grape pomace [8]. Shimojima et al. (2012) studied effect of the USW on rice-powder manufacturing. It was found that the USW crushed the rice into rice-powder differently [9]. Shafiur Rahman, G. M. and Itoh, S. (2011) studied effect of the USW on the natural fibers. The result showed that the treatment of the USW produced micro crack on the fiber surface [5]. Maroušek et al. (2013) investigated the underwater shock waves pressure to enhance oil extraction from Jatropha Curcas L. seeds. It found that the USW created rupture on cell wall which is visualized by the scanning electron microscope (SEM) [6]. Maroušek (2013) studied use of continuous pressure shockwaves apparatus in rapeseed oil processing. The result showed that the use of the USW combination with the mechanical expeller increased oil yields [7]. The USW is more practical and appropriate to apply in such fields, because it is repeatable and easier to control in practices. However, the study of the generation and phenomena of the USW by the HVED or an underwater explosion rather complicated because it used a high quality device such as high speed video [18-19] which is expensive device. Therefore, the CFD simulation is another option to study the phenomena of the USW. However, Nishimura et al. (2010) investigated numerical analysis of the behavior of shock wave in spheroid vessel. It found that discharge phenomenon is difficult to simulate [10] while the electro-hydraulic or the underwater electrical discharge behavior is like the underwater explosion [11]. Therefore, the underwater explosion is preferred in the simulation rather than the underwater HVED and then they are made equivalent. This can be done by transferring the electrical breakdown energy (E_b) into the mass of TNT which is still lacked of a study so far. This is called “the equivalent mass of TNT (W_t)” which is used to fill into the CFD simulation to investigate characteristics and peak pressures of the USW.

This paper aims to investigate characteristics and peak pressure of the USW generated by both methods by the CFD simulation. Peak pressures generated by both methods are predicted and validated by explosive theory [13], experimental [12] and CFD results.

2. Materials and Methods

2.1 Peak pressure estimation for underwater HVED

The peak pressure (P_0) of the underwater HVED which is generated by electrical breakdown discharges through electrodes gap from anode into cathode. After breakdown between gap of both electrodes, the wave is produced this wave is called “shock wave”. The peak pressure of the HVED can be estimated by Equation (1) [12]:

$$P_0 = \frac{9000}{d} E_b^{0.35} \tag{1}$$

where P_0 is the peak pressure in Bar, *d* is the distance of pressure sensor from the center of the discharge or the electrode in millimeters (mm), $E_b = 0.5CV_b^2$ is the electrical breakdown energy in kilo Jules (kJ) and C is the capacitor capacity in Farad (F), V_b is the breakdown voltage in Volt (V).

2.2 Peak pressure estimation for underwater explosion

An explosive detonation is rapidly occurred in water by an explosion of chemical reaction in a substance which releases a hot gas with a pressure shock up to 5 GPa and a temperature about 3000 °C and transmits to the surrounding water and propagating from the explosive point. In the underwater explosion of trinitrotoluene (TNT), the peak pressure (P_m) is estimated by “Cole’s Equation” as shown in Equation (2) [13]:

$$P_m = k_1 \left(\frac{W^{\frac{1}{3}}}{R} \right)^{\alpha_1} \tag{2}$$

where P_m is the peak pressure in megaPascal (MPa), k_1 and α_1 are the constant which depends on explosive charge type. For TNT, the shock parameters are as follows: k_1 =52.16MPa and α_1 =1.13, R is the distance of pressure sensor from the center of the explosive point in meters (m), W is the weight of the explosive charge in kilograms (kg).

2.3 The equivalent mass of TNT (W_t)

In the CFD simulation, the mass of TNT is used as an input parameter for explosion in the simulation. Therefore, the E_b should be converted into mass of the TNT which is called "the equivalent mass of TNT (W_t)" as input in CFD simulation. Due to the Equation (1) and Equation (2) are both for the peak pressure estimation, thus both equations are equal. Therefore, we can derive the W_t in a function of the E_b and the distance of pressure sensor from the explosive point (R) and the center of the discharge (d) as follow:

$$W_t = 1990.652 \left(\frac{R^{1.13}}{d} \right)^{2.6549} E_b^{0.9292} \tag{3}$$

This equation can be used to estimate the W_t for fill in the CFD simulation to predict a peak pressure of the USW.

2.4 Equation of state for water in the CFD simulation

Mie-Gruneisen equation of state for water is used to determine the state of water [15-16]. The pressure of water in compressive state is following in Equation (4):

$$p = \frac{\rho_0 C_0^2 \mu [1 + (1 - (\gamma_0 / 2))\mu - (a/2)\mu^2]}{[1 - (S_1 - 1)\mu - S_2(\mu^2 / (\mu + 1)) - S_3(\mu^3 / (\mu + 1)^2)]^2} + (\gamma_0 + a\mu)e \tag{4}$$

and the pressure of water in expansion state is in the following Equation (5):

$$p = \rho_0 C_0^2 \mu + (\gamma_0 + a\mu)e \tag{5}$$

where μ denotes the condense ratio, $\mu = \eta - 1, \eta = \rho / \rho_0$, η denotes the density ratio of water, ρ denotes the density of water and ρ_0 denotes the initial density of water equal 998kg/m^3 . Water is in a compressed state if $\mu > 0$, and in a expansion state if $\mu < 0$. C_0 denotes the sound-speed; γ_0 denotes Gruneisen coefficient; and *a* represents a volume correction factor; S_1, S_2, S_3 are experimental fitting coefficient; *e* represents the specific energy. The values of the constants for the equation state of water can determine from the CFD simulation [14]. In this simulation, for water, $C_0, \gamma_0, a, S_1, S_2, S_3, e$ are 1640 m/s, 0, 0, 1.921, 0, 0, and 357.1 J/kg, respectively.

2.5 Equation of state for explosive detonation in the CFD simulation

For the explosive detonation, the CFD simulation is using model standard Jones, Wilkins, and Lee (JWL) Equation of state to determine the pressure of detonation [15-17]. It can be written in the Equation (6):

$$p = A\left(1 - \frac{\omega\eta}{R_1}\right)e^{-(R_1/\eta)} + B\left(1 - \frac{\omega\eta}{R_2}\right)e^{-(R_2/\eta)} + \omega\eta\rho_0 e \tag{6}$$

where $A, B, R_1, R_2, and\ \omega$ are constants related to the state of the explosives; η denotes the ratio of the density of explosion gas to that of initial explosives, $\eta = \rho / \rho_0$, ρ denotes the density of explosive and ρ_0 denotes the initial density of explosive equal 1630kg/m^3; *e* denotes specific internal energy equal

4.29×10^6J/kg. The values of the constants for the equation state of TNT can determine from the CFD simulation [14]. In this simulation, for TNT explosive charge, are 3.7377e11Pa, 3.747e9Pa, 4.15, 0.9, and 0.35, respectively.

2.6 CFD simulation set up

In this paper, the model is 2D-axisymmetric and with the wedge shape as shown in Figure 1. The angle of the wedge is defined by the CFD simulation. Only wedge inner radius and outer radius needs to be defined. A domain of the wedge is shown in figure 1 which inner radius and outer radius are 0.1 and 800 mm, respectively. An influence of reflection on the wall at the pressure distance from the center of the explosion of 345, 445, and 555 mm is neglected by the wedge that is 800 mm long.

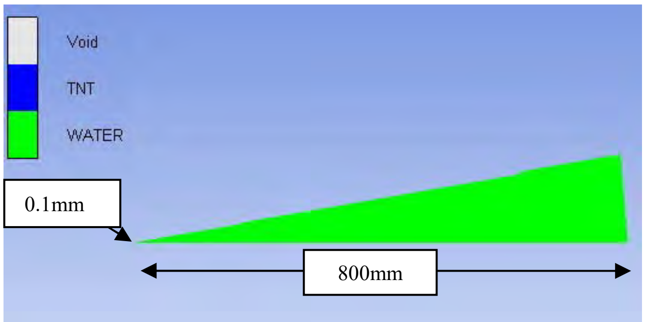

Figure 1 The model set up of the wedge shape

The charge size of TNT depends upon equation (3) which the E_b range is various from 2.5-30 kJ. The mesh of the wedge model which is used in this paper is quadrilateral [15] element and defined by the CFD simulation. The mesh dependence is performed by varying the mesh size from 0.0078125 to 1mm by increment as follows: 0.0078125, 0.015625, 0.03125, 0.0625, 0.125, 0.25, 0.5, and 1mm, respectively.

The charge size of TNT which is in radius for fill in the CFD simulation can determine from Equation (3) in the W_t. After obtaining the W_t, the charge size of TNT can be determined from Equation (7):

$$W_t = \rho V \qquad (7)$$

where ρ is the density of TNT equal 1630kg/m^3, V is the volume of the charge size of TNT = $(4/3)\pi R^3$. In the CFD simulation, the charge size of TNT which is the detonation point is located at the coordinate (0, 0) is shown in Figure 2. The gauge which is used to measure peak pressure is located at 345mm from the center of explosive point is also shown in Figure 2.

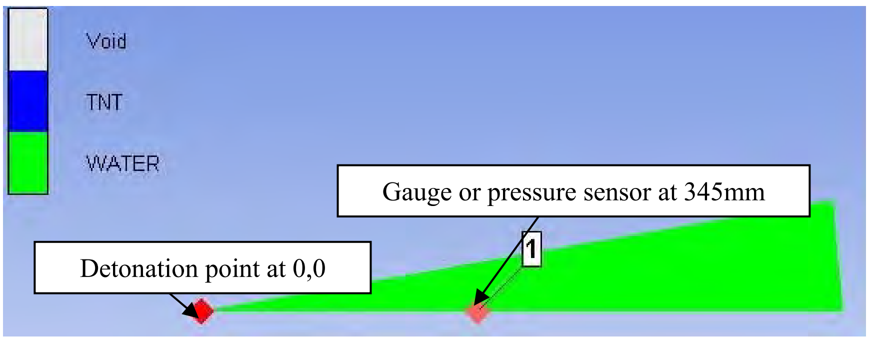

Figure 2 Location of the charge size and gauge point

3. Results and Discussions

3.1 Mesh size dependence

The Figure 3 shows the peak pressure of the CFD simulation results of the E_b =2.5 kJ and the mesh size dependence are also compared with Equation (2). It was found that the result of the refined mesh at 0.0078125 mm is the closest one with the Equation (2) with an error of 10.79 % as shown in Table 1. From Figure 3, if the mesh size is smaller, the peak pressure becomes closer to Cole's Equation (2). Therefore, in this study, the 0.0078125 mm is used, because the limitation of the computing power and the time, while the error is acceptable at around 10%. However, the smaller mesh size to verify the mesh independence and the saturation of the CFD results should be performed in the near future.

Table 1 Error comparison between mesh size and Cole's Equation of the E_b =2.5kJ at 345mm from the center of explosion

Mesh size (mm)	Peak pressure (MPa)		Error (%)
	CFD	Cole's Equation (2)	
0.0078125	3.249	3.642	10.79
0.015625	3.084	3.642	15.32
0.03125	2.883	3.642	20.84
0.0625	2.616	3.642	28.17
0.125	2.309	3.642	36.60
0.25	2.005	3.642	44.95
0.5	1.778	3.642	51.18
1.0	1.361	3.642	62.63

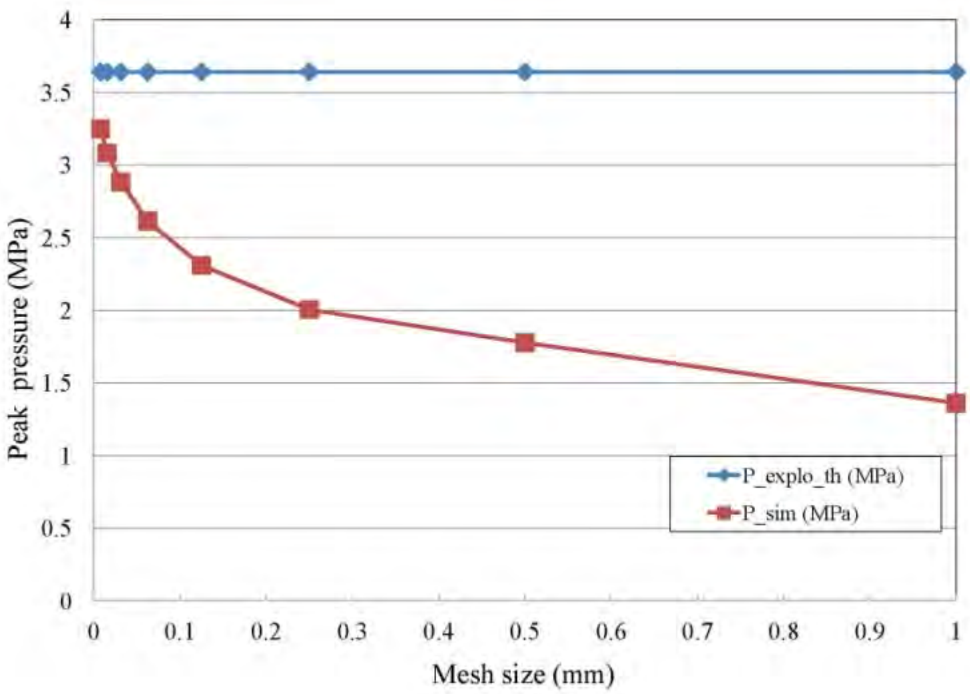

Figure 3 The mesh size dependence at the E_b =2.5kJ

The figure 4 (a)-(d) shows the peak pressure propagation on times of the USW that predicted by the CFD simulation of the E_b =2.5kJ. The peak pressure of the refined mesh size at 0.0078125mm located at the distance of pressure gauge at 345mm is 3.249MPa.

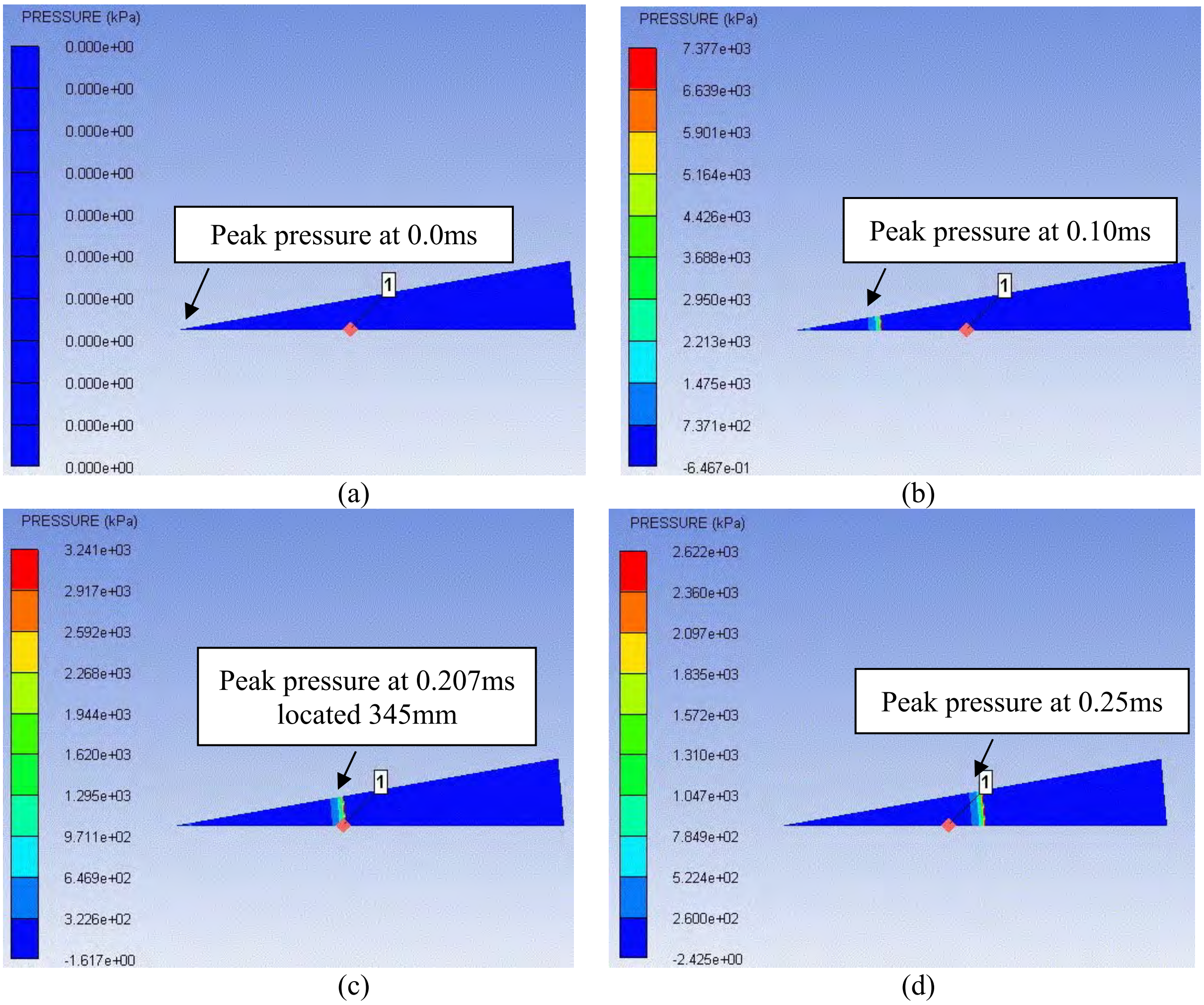

Figure 4 Peak pressure propagation on times of the refined mesh size 0.0078125mm of the E_b =2.5kJ at 345mm (a) 0.00ms, (b) 0.1ms, (c) 0.207ms, and (d) 0.25ms

3.2 The peak pressure prediction and validation

The peak pressure of the explosive theory [13], experimental [12] and the CFD simulation results are shown in Figure 5-7 which is measured at the location from the center of explosive point and various the E_b are 345, 445, 555mm, and 2.5-30kJ, respectively.

The Figure 5 shows the peak pressure that predicted by the CFD simulation which is also close to the explosive theory, and experimental. The peak pressure range of 32-81 Bar at 345mm. From Figure 5 the trend of equation $y = 22.856x^{0.373}$ is similar to the trend of the experimental [12] where *y* is the peak pressure and *x* is the E_b.

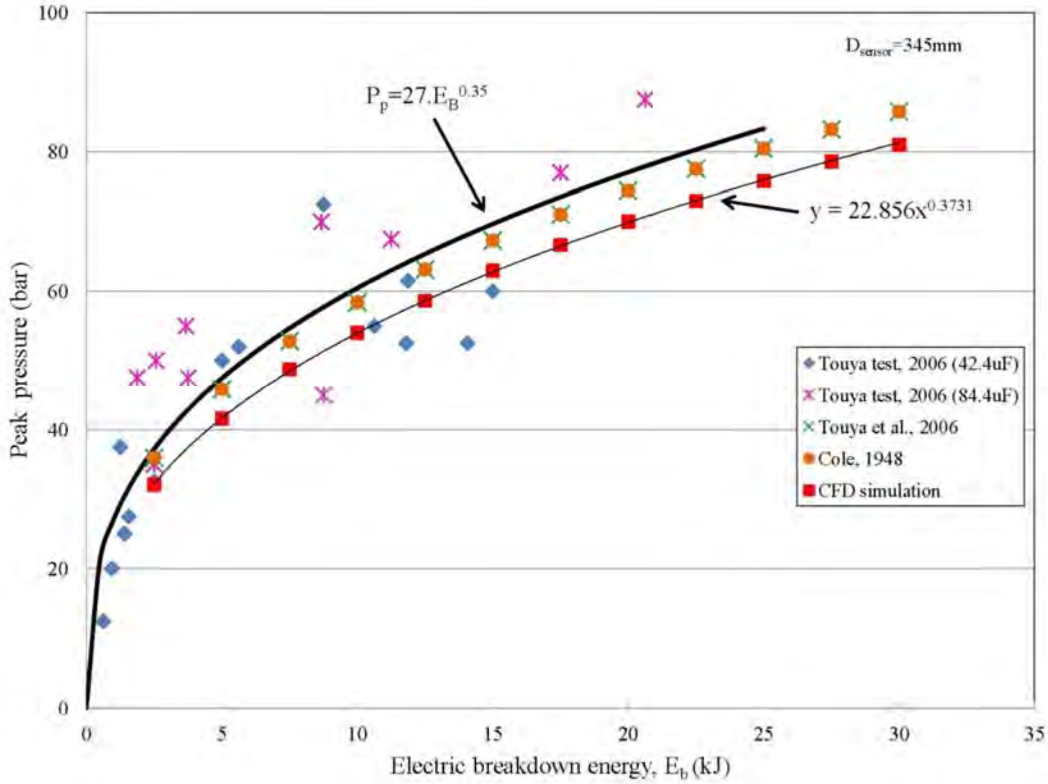

Figure 5 Peak pressure at 345mm from explosion point

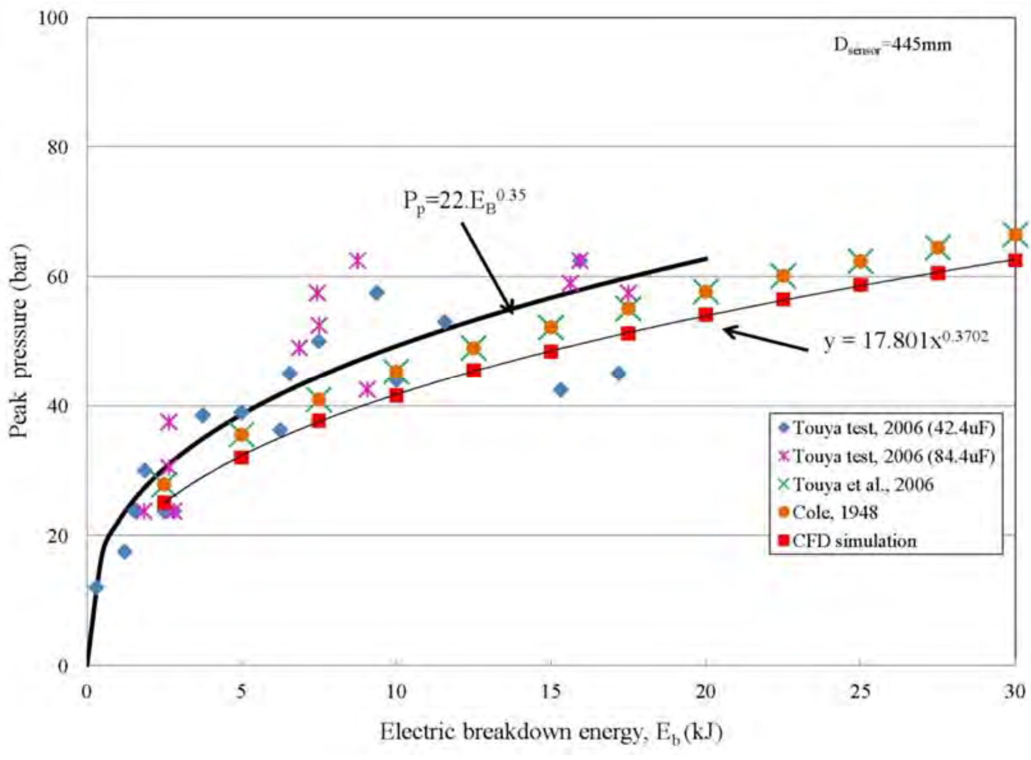

Figure 6 Peak pressure at 445mm from explosion point

In addition, the peak pressure predicted by the CFD simulation shown in Figure 6 is also close to the explosive theory [13], and experimental [12]. The peak pressures are ranged from 25-62.5 Bar at distance of 445 mm. From the Figure 6 the trend of equation $y = 17.801x^{0.3702}$ is also close to the trend of the experimental [12].

Moreover, In Figure 7 shown the peak pressure predicted by the CFD simulation which is also close to the explosive theory [13], and experimental [12]. The peak pressures are ranged from 20-49.9 Bar at distance of 555mm. From the Figure 7 the trend of equation $y = 14.535x^{0.363}$ is similar to the trend of the experimental [12].

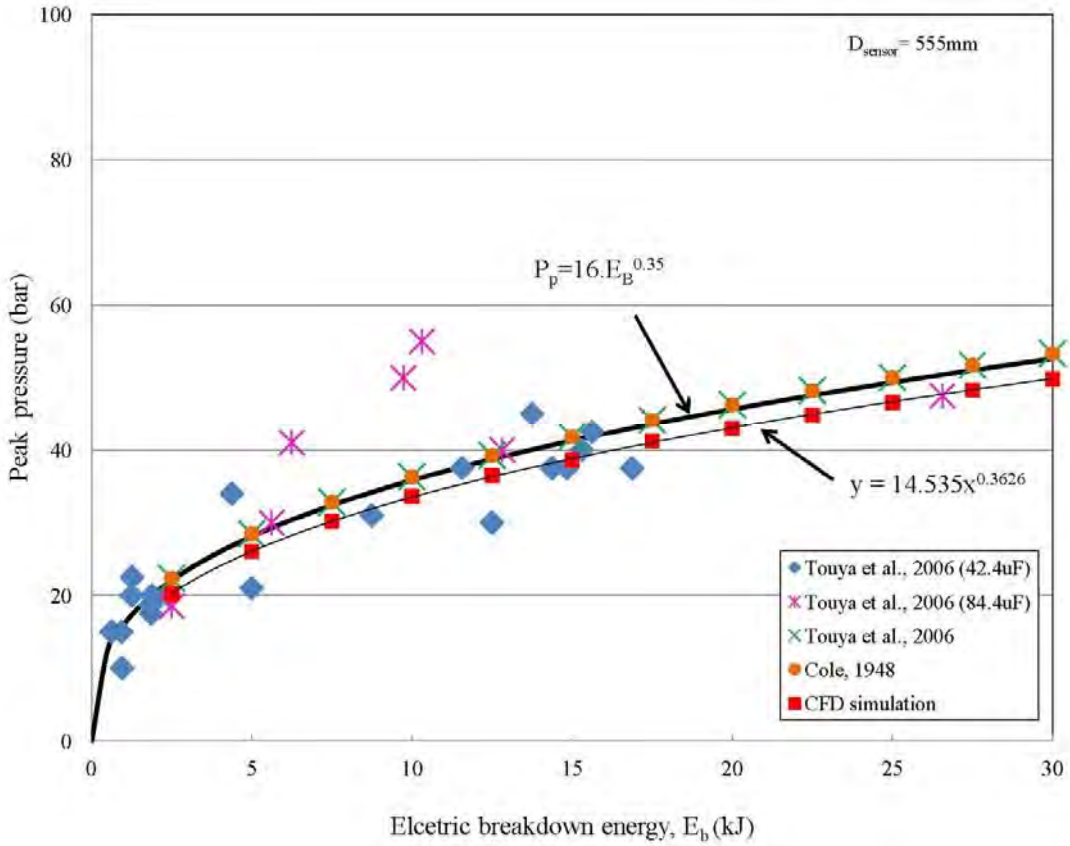

Figure 7 Peak pressure at 555mm from explosion point

3.3 The error of the CFD simulation peak pressure prediction comparison Cole's Equation

The error of peak pressure predicted by the CFD simulation at various E_b at different distance of pressure sensor from the center of the explosive point are 345, 445, and 555mm, respectively, compared with the theory of explosion are range 5.53-10.79%, 5.96-9.98%, and 6.49-9.66% shown in the Figure 8. This result found that far away from the center of explosion point, the peak pressure is close and decrease to Cole's Equation or explosive theory [13] results as follows 10.79, 9.98, and 9.66%, respectively, which is agreement with other research [8, 12, 15]. Moreover, the E_b increases but the error decreases shows in Figure 8. Because the distance of pressure sensor (d, R) is a function of the E_b and peak pressure shown in Equation (1) and Equation (2), then the farthest distance gives the smallest.

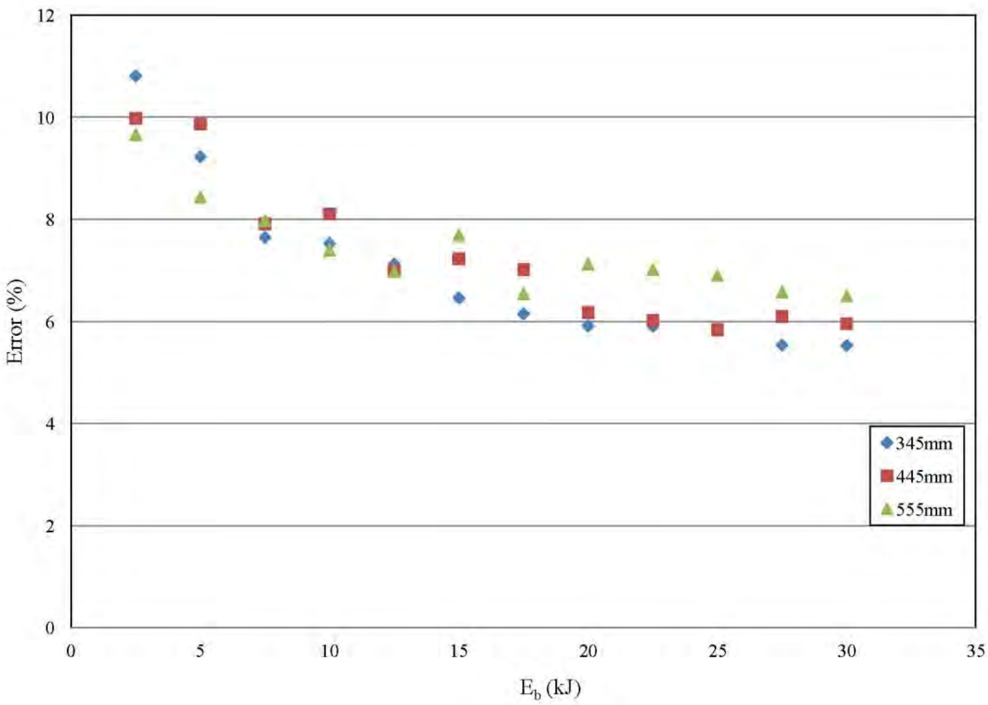

Figure 8 The error of CFD simulation at various the E_b compared Cole's Equation

4. Concluding Remarks

In this paper, the W_t in Equation (3) can be obtained by equivalent with the E_b and is used as the input parameter in the CFD simulation. The underwater peak pressure at various distances from the centre of the explosive detonation point which is 345, 445, and 555mm, respectively, when the E_b range 2.5-30kJ is predicted. It is found that the peak pressure predicted by the CFD simulation are in the range of 32-81 Bar, 25-62.5 Bar, and 20-49.9 Bar, at distance of 345, 445, and 555mm, respectively. The trends of peak pressure are well agreed with the explosive detonation theory and experiments. Errors of the peak pressure predicted by the CFD simulation compared Equation (2) are about 5-11%. In addition, the CFD simulation results are also close to previous experimental results. Therefore, it is confirmed that the proposed methods is reliable and effective to use to study of the USW. This method will be useful for further investigation or facility design.

Acknowledgement

The author would like to thank the Department of Mechanical Engineering, Ubon Ratchathani University for support of research and the Rajamongala University of Technology Isan for the scholarship of Ph.D. study.

References

[1] Hosseini, S.H.R., Iwasaki, S., Sakugawa, T., and Akiyama, H 2011 *Journal of the Korean Physical Society*. **59** 3526.
[2] Alvarez, U.M., Loske, A.M., Castaño-Tostado, E., and Prieto, F.E 2004 *Innovative Food Science and Emerging Technologies*. **5** 459.
[3] Boussetta, N., Ferron, A.De., Reess, T., Pecastaing, L., Lanoisellé, J.L., and Vorobiev, E 2009 *Proc. the 17th IEEE International Pulsed Power Conference* (Washington, D.C., USA.) p 1108.
[4] Maroušek, J 2014 *Industrial Crops and Products*. **53** 1.
[5] Shafiur Rahman, G. M. and Itoh, S 2011 *Fibers and Polymers*. **12** 121.
[6] Maroušek, J., Itoh, S., Higa, O., Kondo, Y., Ueno, M., Suwa, R., Komiya, Y., Tominaga, J., and Kawamitsu, Y 2013 *Biotechnology & Biotechnological Equipment*. **27** 3654.

[7] Maroušek, J 2013 *Clean Technologies and Environmental Policy*. **15** 721.
[8] Boussetta, N., Vorobiev, E., Reess, T., De Ferron, A., Pecastaing, L., Ruscassié, R., and Lanoisellé, J.-L 2012 *Innovative Food Science and Emerging Technologies*. **16** 129.
[9] Shimojima, K., Miyafuji,Y., Naha, K., Higa, O., Matsubara, R., Higa, K., Higa, Y., Matsui, T., Takemoto, A., Tanaka, S., Maehara, H., and Itoh, S 2012 *the International Journal of Multiphysics.* **6** 355.
[10] Nishimura, Y., Kawaji, N., and Itoh, S 2010 *the International Journal of Multiphysics*. **4** 317.
[11] Mamutov, V., Golovashchenko, S., and Mamutov, A 2014 *Proc. 13th International LS-DYNA Users Conference, Session: Metal Forming* (Detroit, USA.) p 1-1.
[12] Touya, G., Reess, T., Pécastaing, L., Gibert, A., and Domens, P 2006 *Journal of Physics D: Applied Physics.* **39** 5236.
[13] Cole, R.H. 1948 Underwater Explosions (Princeton, New Jersey)
[14] Century Dynamics Inc. 2003 AUTODYN theory manual version 4.3 (Concord, CA.)
[15] Jha, N. and Kiran Kumar, B. S 2014 *International Journal of Science and Research*. **3** 1162.
[16] A-mana, Z., Wen-shan, Y., and Xiong-liang, Y 2012 *Applied Ocean Research*. **34** 10.
[17] Wang, G., Zhang, S., Yu, M., Li, H., and Kong, Y 2014 *Applied Ocean Research*. **46** 40.
[18] Shibuta, M., Hamashima, H., and Itoh, S 2010 *the International Journal of Multiphysics* 241.
[19] Higa, O., Matsubara, R., Higa, K. Miyafuji, Y., Gushi, T., Omine, Y., Naha, K., Shimojima, K., Fukuoka, H., Maehara, H., Tanaka, S., Matsui, T., and Itoh., S 2012 *the International Journal of Multiphysics*. **6** 89.